

N 7 3 - 1 2 0 2 7

**NASA TECHNICAL  
MEMORANDUM**

**NASA TM X-68161**

**NASA TM X-68161**

**CASE FILE  
COPY**

**FLYOVER AND STATIC TESTS TO INVESTIGATE EXTERNAL FLOW EFFECT ON  
JET NOISE FOR NON-SUPPRESSOR AND SUPPRESSOR EXHAUST NOZZLES**

by Richard R. Burley and Raymond J. Karabinus  
Lewis Research Center  
Cleveland, Ohio

TECHNICAL PAPER proposed for presentation at  
Eleventh Aerospace Sciences Meeting and Technical Display sponsored  
by the American Institute of Aeronautics and Astronautics  
Washington, D. C., January 10-12, 1973

FLYOVER AND STATIC TESTS TO INVESTIGATE EXTERNAL FLOW EFFECT ON  
JET NOISE FOR NONSUPPRESSOR AND SUPPRESSOR EXHAUST NOZZLES

Richard R. Burley and Raymond J. Karabinus

Lewis Research Center  
National Aeronautics and Space Administration  
Cleveland, Ohio

Abstract

At the relatively high takeoff speeds of supersonic transport aircraft, external air flowing across the exhaust nozzles may affect their jet noise characteristics. To investigate this, a series of flyover and static tests were conducted using an F-106B aircraft modified to carry two underwing nacelles each containing a calibrated J85-GE-13 turbojet engine. A flyover altitude of 300 feet and a Mach number of 0.4 provided acoustic data that were repeatable to within  $\pm 1.5$  PNdB. Comparisons of flyover and static data indicated that external flow reduced the noise of an auxiliary inlet ejector nozzle. An unsuppressed plug nozzle was not affected whereas the plug suppressor configurations were not as effective in flight.

Introduction

During takeoff of supersonic transport aircraft, the dominant noise source is the high velocity jet issuing from the exhaust nozzle. Investigation of the noise of suitable exhaust nozzles generally has been done at static conditions (c.f., ref. 1). However, when the maximum sideline noise is reached during takeoff of advanced supersonic cruise configurations, the forward speed of the aircraft can be as high as Mach 0.35. At these relatively high takeoff speeds, external air flowing across the exhaust nozzles could significantly affect their noise characteristics since the entrainment and mixing of external flow with the high velocity jet could be altered.

To gain some insight into this phenomenon, a series of both flyover and static tests are being conducted on exhaust nozzles with and without noise suppressor devices. The tests were made with an F-106B aircraft modified to carry two underwing nacelles each containing a calibrated J85-GE-13 turbojet engine. The flyovers were conducted at an altitude of 300 feet and a Mach number of 0.4 and acoustic measurements were taken from a ground station directly beneath the flight path. For static tests, the acoustic measurements were taken at a radial distance of 100 feet from the nozzle.

A variety of basically different nozzle concepts are being used in this flight program. Some of these results are reported in Ref. 2. The present paper will present preliminary results for additional configurations. Two of the unsuppressed nozzles were the auxiliary inlet ejector and the conical plug. Both of them approximated the geometry appropriate for low-speed operation of variable nozzles designed for efficient operation in the Mach 2.7 range. Two of the suppressor nozzles consisted of a 12-chute and a 48-tube configuration which were installed on the conical plug nozzle. This paper will present a preliminary analysis of external flow effects on the acoustic and thrust characteristics for these exhaust nozzles.

Test Facility

The flyover tests as well as some of the static tests were conducted with an F-106B aircraft modified to carry two underwing nacelles. The aircraft in flight is shown in Fig. 1. A schematic view of the nacelle-engine installation is shown in Fig. 2. The 25-inch diameter nacelles were located at approximately 32 percent semispan with the exhaust nozzles extending beyond the wing trailing edge. Since the nozzles would interfere with normal elevon movement, a section of the elevon immediately above each nacelle was cut out and rigidly fixed to the wing. Each nacelle contained a calibrated J85-GE-13 afterburning turbojet engine. The nacelles had normal shock inlets with blunted cowl lips for the flyover tests. Secondary air to cool the engine and afterburner was supplied from the inlet and was controlled at the periphery of the compressor face by a rotary valve. For the static tests, the blunted cowl lips were replaced with a bellmouth and the secondary air was supplied from an external source. A load cell technique (ref. 3) was used to measure nacelle thrust minus drag to determine exhaust nozzle performance for both static and flyover tests.

Engine airflow was obtained using the calibration techniques of Ref. 4 along with measurements of engine speed and total pressure and temperature at the compressor face. Fuel flows were obtained from flow meters. Conditions at the primary nozzle exit were computed knowing airflow, turbine discharge conditions and fuel flow rates.

A calibrated test boom located on the aircraft nose was used to determine free-stream static and total pressure, aircraft angle-of-attack, and yaw angle. Aircraft altitude was determined using an onboard radio altimeter and a barometric altimeter along with ground-based radar. Aircraft speed was obtained from a Mach meter. An onboard digital data system recorded pressures, temperatures, and load cell output on magnetic tape.

Noise Measurements

Microphones for both static and flyover tests were 1-inch diameter ceramic type. Their frequency response was flat to within  $\pm 2$  dB for grazing incidence over the frequency range used (50 to 10,000 Hz). The output of the microphones was recorded on a two channel direct record tape recorder. The entire system was calibrated for sound level in the field before and after each test with a conventional discrete calibrator.

Both the flyover and static signals were recorded on magnetic tape. The tape was played back through one-third-octave-band filters and then reduced to digital form. The averaging time for data reduction was 0.1 second for the flyover signal and 0.125 second for the static signal.

Meteorological conditions, in terms of dry-bulb and dew point temperatures, wind speed and direction, and barometric pressure were recorded periodically throughout the tests. Wind speeds were less than 10 knots during all tests.

#### Flyover Tests

Noise measurements for the flyover tests were made from a ground station directly beneath the flight path as shown in Fig. 3. A primary and a backup microphone were used. The primary microphone, which was fitted with a windscreen that caused no loss of signal, was positioned 4 feet above a concrete surface. The backup microphone was positioned on the concrete surface. Both microphones were oriented to receive the acoustic pressure waves at grazing incidence. The flyover results in this report were recorded using the primary microphone.

The flyovers were conducted at an altitude of 300 feet and a Mach number of 0.4. The main engine of the aircraft (a J-75) was at idle power as the data were recorded. The J85 engine in the nacelle containing the research nozzle was operated over a range of power settings and the J85 engine in the other nacelle was shut off and allowed to windmill. To compensate for the asymmetric power (i.e., one J85 at high power and the other off) and maintain a very low yaw angle ( $1^\circ$  or less), the aircraft was in a slightly banked attitude as it flew over the measuring station. A 400 Hz signal was put on the tape by a ground-based observer stationed at the microphone to indicate when the aircraft was directly over the microphone.

In the selection of a flyover altitude, it is desirable from a noise standpoint to conduct the flyovers at a low altitude. Otherwise, the propagation distance from the noise source to the microphone becomes quite long making it difficult to obtain meaningful noise data. However, it is also necessary for the altitude to be high enough to be consistent with safe operation of the aircraft.

To determine a reasonable compromise in altitude, flyovers were conducted at altitudes of 1200, 600, and 300-ft. Typical results illustrating the change in perceived noise level with time are shown in Fig. 4 for an unsuppressed nozzle at maximum afterburner power setting of the J85 engine. At the highest altitude, the data scatters too much to give meaningful results. Decreasing the altitude to 600-ft., reduces the scatter but it is still difficult to accurately define the peak noise level or the time it occurs. An altitude of 300-ft provides acoustic data that is repeatable to within  $\pm 1.5$  PNdB and hence was used for the subsequent testing.

#### Static Tests

The static data for the auxiliary inlet ejector nozzle used in this report was obtained from an isolated nacelle and previously was reported in Ref. 1. Additional static data for the plug nozzle and the suppressors were obtained with the nacelle mounted on the aircraft.

The location of the microphone for these static tests is shown in Fig. 5. The microphone was positioned 4 feet above the concrete surface and was oriented to receive the acoustic pressure waves at normal incidence. It was fitted with a windscreen that caused no loss of signal. The acoustic measure-

ments were taken at a radial distance of 100 feet from the nozzle exit in increments of  $10^\circ$  over a  $90^\circ$  sector. During the measurements, the main J-75 engine was at idle conditions. The J85 engine in the nacelle containing the research nozzle was operated over a range of power settings and the J85 engine in the other nacelle was shut off.

#### Exhaust Nozzles

##### Nonsuppressor Types

One of the unsuppressed nozzles tested was the auxiliary inlet ejector (AIE) nozzle shown in Fig. 6. It incorporated a series of 16 auxiliary inlet doors located around the periphery of the external skin ahead of the primary nozzle. The principal purpose of the doors is to allow outside air to enter the ejector and help prevent overexpansion of the primary jet at low values of nozzle pressure ratio such as those that exist at takeoff. The present configuration had the doors fixed in the  $16^\circ$  position. The aft portion of the nozzle simulated the closed position which is also characteristic of low pressure ratio operation. Additional details of this nozzle design are given in Ref. 5.

Another unsuppressed nozzle tested was the plug nozzle shown in Fig. 7. It consisted of a  $10^\circ$  half-angle conical plug body and a primary flap with a  $14^\circ$  trailing edge. A plug nozzle generally has a translating outer shroud, which, for efficient operation at low pressure ratios, is retracted. The present configuration simulates the shroud in this position. Further details of this nozzle design are given in Ref. 6.

##### Suppressor Types

The suppressor configurations were installed on the conical plug nozzle just discussed. The geometric throat for the suppressor configurations was at about the same location on the plug surface as the exit plane of the primary flap for the conical plug nozzle. A plug nozzle was selected for these suppressor tests because it provides good aerodynamic performance, its mechanical systems are relatively simple, and the plug body provides a place to store retractable noise suppressors.

One of the suppressor nozzles tested was the 12-chute configuration shown in Fig. 8. External air flows down the smoothly converging surfaces of the 12 chutes, and mixes with the primary jets issuing from the 12 rectangular shaped exits. Since this suppressor design is relatively bulky, it was presumed to be nonretractable. The area ratio, that is the area circumscribing the mixing nozzle divided by the primary exit area is 3. Some acoustic and performance results are given in Ref. 2. Performance of an 8-1/2 inch diameter cold flow isolated model at both takeoff and supersonic cruise conditions is given in Ref. 7. At supersonic cruise this type of suppressor caused a 1-1/2 percent loss in gross thrust which may be excessive for most applications.

Another suppressor nozzle tested was the 48-tube configuration shown in Fig. 9. This configuration has a blunt base. The tubes were arranged in 6 clusters, called nozzle boxes, and each nozzle box contained 8 tubes. For each nozzle box, the area ratio was 2.5. The tubes were 4 inches long which resulted in a ventilation factor (ratio of side

flow area to base area per nozzle box) of 0.3. There were also six triangular shaped openings (one opening between each of the nozzle boxes) through which about 33 percent of the primary flow is discharged.

A major consideration dictating the shape of this configuration was that, in concept, the tubes must be storable inside the plug body. Three of the nozzle boxes would slide inward and forward on tracks and be stored forward in the plug. The other three nozzle boxes would fold into the plug by means of a pivot. The nozzle box side walls would then cover the tubes and become part of the plug surface. This storable concept imposed limitations on the configuration which may have degraded its acoustic and thrust performance.

#### Adjustments to Measured Spectra

To determine whether differences exist between the flyover and static data, the measured spectra were adjusted to comparable conditions which were 100 ft from the nozzle in the free field and on a standard day of 77° F and 70 percent relative humidity. The standard day adjustment was made using the simplified procedure of FAR 36 (ref. 8). The adjusted flyover and static spectra would then be directly comparable. The following discussion provides the details of these adjustments.

#### Static

Static data for the AIE nozzle was taken with an isolated nacelle over a grassy surface and data for the other nozzles were taken on the aircraft over a concrete surface. Each required a different method to make the free-field adjustment. The adjustment from concrete to free-field was based on the assumption that the concrete surface was a perfect reflector and that the jet noise was a single point source (ref. 9). The theoretical curve was modified by a smooth curve tangent to the theoretical curve at the low and high frequencies (fig. 10(a)). This gross adjustment resulted in reducing the magnitude of the spectra by about 6 dB at the low frequencies and 3 dB at the high frequencies.

The adjustment from grass to free field was done by first adjusting the data from grass to concrete and then adjusting it from concrete to free field. The adjustment from concrete to free field has just been described. The adjustment from grass to concrete was based upon data from a cylindrical ejector nozzle that was tested over both surfaces. The spectra along with a schematic of this nozzle are shown in Fig. 10(b). There was a large difference only in the mid frequencies. Therefore, the spectrum taken over grass was adjusted to that taken over concrete by connecting the lower and upper segments of the measured spectrum with a smooth curve of the same shape as predicted by SAE. The resulting OASPL and PNL values for the spectrum adjusted from grass to concrete are about the same as those for the spectrum taken over concrete. This adjustment from grass to concrete was applied only to the auxiliary inlet ejector nozzle. In doing so it was assumed that its spectral shape was similar to that of the cylindrical ejector. This adjustment was not made to the plug and its suppressor nozzles since they were tested over concrete.

Further evidence of the validity of the adjustment from grass to concrete is shown in Fig.

10(c). Here the results for the plug nozzle over a concrete surface are compared to that of a similar nozzle over a grass surface (from ref. 1). The spectra adjusted in both cases to free field and standard day by the above procedures are compared in the figure. There is good agreement between the spectra except in the vicinity of 200 and 1600 Hz. The reason for the dip at 200 Hz is not yet known, but the dip at 1600 Hz is attributed to destructive interference. The resulting OASPL and PNL values for the spectra are within 2 dB of each other.

The last adjustment was for microphone orientation. The static data were taken with the microphone oriented to receive the acoustic waves at normal incidence. The data were adjusted to that obtained if the microphone had been oriented for grazing incidence which is the orientation of the microphone for flyover data. The adjustment resulted in reducing the amplitude of the static spectrum at frequencies above 2000 Hz, varying from 0.1 dB at 2500 Hz to 4 dB at 10,000 Hz.

#### Flyover

During the flyover, the direct ray distance from the nozzle to the microphone continuously changes (Fig. 11(a)). The angle between the direct ray and the jet exit centerline, referred to as the acoustic angle, also changes (see Fig. 11(a)). The spectra were adjusted to a constant distance of 100-ft (see Fig. 11(b)). The adjustment was made accounting for inverse-square radiation and atmospheric attenuation. The resulting increase in sound pressure level is indicated on Fig. 11(b) (from spectrum (1) to (2)). The level at (1) represented the spectrum after it had been adjusted to free-field and standard day conditions. Adjustment to free-field conditions was done in a manner similar to that for the static data taken over concrete.

Another adjustment to the flyover data was necessary because the noise source is in motion relative to the microphone resulting in a Doppler shift of frequency. The best way to apply the Doppler shift to jet noise is not clear because the principal source of noise is distributed over a significant length of the jet downstream of the nozzle which is not necessarily moving uniformly relative to the aircraft speed. The approach used here was simply to shift all the frequencies by the same amount based on the speed of the aircraft. This amounted to shifting the frequencies by one 1/3-octave band at the most. Results are shown in Fig. 11(b). This shift results in a change of bandwidth and, according to Ref. 10, a correction should be made to the level of the shifted spectrum to maintain the correct power spectral density. For the aircraft conditions, this correction would not significantly change the level and so it was not applied. According to Ref. 2 there is another part of the Doppler shift, termed dynamic effect. Application of the dynamic effect would have significantly changed the level of the flyover spectra.

#### Results and Discussion

##### Acoustic Characteristics

Comparison of the adjusted flyover and static spectra for each of the four nozzles is shown in Figs. 12 through 15 for a relative jet velocity of 1970 fps and for the acoustic angle that resulted in peak flyover noise. In making the comparisons,

the greatest emphasis should be placed on the data at frequencies between 160 and 5000 Hz. At frequencies below 160 Hz, the short integration time (0.1 sec), the rapidly changing conditions of the flyover, and the narrowness of the frequency bands combine to give results that are not reliable. At frequencies above 5000 Hz, the acoustic signal received at the ground station quite possibly is below the noise floor of the recording equipment (ref. 11). Values of the atmospheric absorption coefficient are very large at these high frequencies and multiply the noise floor to unrealistically high noise levels in correcting the data to 100 ft. The absorption coefficients are also difficult to evaluate and prone to error (ref. 12).

Comparison of flyover and static spectra for the plug nozzle is shown in Fig. 12. The flyover spectrum is below the static spectrum from 160 to 800 Hz and above it from 800 to 5000 Hz. This resulted in an OASPL value and a PNL value that was about the same for the flyover as for the static spectrum. This good agreement between the spectra suggests that external flow probably did not significantly affect the noise of the plug nozzle.

Comparison of the flyover and static spectra for the auxiliary inlet ejector nozzle is shown in Fig. 13. The flyover spectrum is lower than the static spectrum over the entire frequency range of primary interest. Furthermore, the magnitude of the differences is considerably greater than for the plug nozzle. This results in an OASPL value about 9 dB lower and a PNL value of 8 PNdB lower for the flyover than the static spectrum. This suggests that external flow had a beneficial effect on the noise of the auxiliary inlet ejector nozzle. It is probably caused by a difference in the amount of outside air that enters the ejector through the auxiliary inlet doors at flyover conditions compared to static conditions.

Comparison of flyover and static spectra for the 12-chute suppressor nozzle is presented in Fig. 14. The flyover spectrum is markedly higher than the static spectrum over most of the frequency range of interest. The largest differences occur between frequencies of 630 and 1600 Hz. This resulted in an OASPL value about 6 dB higher and a PNL value about 5 PNdB higher for the flyover than the static spectrum. This suggests that external flow had an adverse effect on the suppression characteristics of this nozzle.

Comparison of flyover and static spectra for the 48-tube suppressor nozzle is shown in Fig. 15. The flyover spectrum is only slightly higher than the static spectrum except at frequencies between 1250 and 2000 Hz. This resulted in an OASPL value only about 3 dB higher and a PNL value only about 2 PNdB higher for the flyover than for the static spectrum. The agreement between the spectra is quite good suggesting that the adverse effect of external flow was not as great as it was for the 12 chute suppressor.

Flyover noise levels and directivity for the four nozzles are shown in Fig. 16 along with the background noise level which was obtained during a flyover with the J85 engines windmilling. In the region of primary interest, which is between acoustic angles of about 90° and 20°, the background noise level is sufficiently low so it has

no effect on the results. Also shown in this figure is a table comparing the acoustic angle at which the peak noise occurred during flyover at the 300-ft altitude to that predicted from static data extrapolated to a 300-ft sideline. The table also shows the difference in peak noise between that predicted using static results and that obtained during the flyover.

The plug nozzle was the noisiest in flyover having a peak value of 119 PNdB at an acoustic angle of 45°. The static results correctly predicted the angle at which the peak noise occurred. However, the predicted value for the peak noise level was somewhat low. The 12-chute suppressor nozzle, which had the sharpest peak, had a peak noise level of 117.5 PNdB occurring at an angle of 50°. Static results predicted a slightly lower peak noise level occurring at an acoustic angle of 55°. The 48-tube suppressor nozzle, which had the flattest peak, had a peak noise level of 116 PNdB. It occurred the farthest away from the jet axis of the nozzles tested, 70°. The static results correctly predicted both the peak noise level and the associated acoustic angle. The auxiliary inlet ejector nozzle was the quietest nozzle tested in flyover. It had a peak noise level of 114.5 PNdB that occurred at an angle of 40°. This is considerably different from the static results which predicted a much higher peak noise level, about 9 PNdB higher, occurring farther away from the jet axis, 50°. The directionality shift is partly responsible for the flyover noise being lower than that predicted from the static data.

#### Performance Characteristics

In addition to acoustic characteristics, performance characteristics are also important. Performance characteristics of all four nozzles at static and flyover conditions, is presented in Fig. 17. Performance is given in terms of nozzle gross thrust coefficient, defined as measured thrust minus drag divided by ideal thrust of the primary jet. The plug nozzle had the highest performance at static conditions, 0.995. For flyover conditions, the performance decreased to 0.965 probably due to increased friction and pressure drag on the external surfaces of both the primary flap and the boattail. The auxiliary inlet ejector nozzle also had high performance at static conditions, 0.985. In addition, there was no loss in performance from static to flyover conditions. This is probably because the increase in external drag is compensated for by an increase in internal performance as more external air enters the ejector through the auxiliary inlet doors.

The noise suppressor nozzles were the type that divided the primary jet into a number of smaller jets. This increased the wetted area (excluding base area) of these nozzles which tends to reduce the thrust by increasing both the internal flow losses and the external skin friction drag. Another source of drag is that caused by unventilated base areas. The performance of the 12-chute suppressor is 0.925 at static conditions. No significant reduction in performance occurred from static to flyover conditions. This suggests that the base area was ventilated for both static and flyover conditions probably because the chutes have smoothly converging external surfaces rather than blunt surfaces. The 48-tube suppressor had the lowest performance, 0.91 at static conditions and decreased

to 0.865 for flyover conditions. The reduction in performance from static to flyover conditions is probably due to an increase in external pressure drag on the base area caused by the nozzle having a blunt base.

### Conclusions

(1) A flyover altitude of 300-ft provided acoustic data that was repeatable to within  $\pm 1.5$  PNdB.

(2) The auxiliary inlet ejector nozzle was the quietest in flyover and the plug nozzle was the noisiest. The difference was about 4-1/2 PNdB.

(3) Comparison of the adjusted spectra indicated that external flow appears to reduce the noise of an auxiliary inlet ejector nozzle. The unsuppressed plug nozzle was not affected whereas the plug suppressor configurations were not as effective in flight. The adverse effect was greater for the chute suppressor than for the tube suppressor.

(4) The auxiliary inlet ejector nozzle had the highest thrust performance at flyover conditions, 0.985. Its performance at static conditions was the same as for flyover. The 48-tube suppressor nozzle had the lowest performance and dropped from 0.91 at static conditions to 0.865 at flyover conditions.

### Symbols

D	sum of nozzle external pressure and skin friction drags
dB	decibel
F	nozzle gross thrust
F <sub>ip</sub>	ideal thrust of primary jet
Hz	hertz (cycles per second)
OASPL	overall sound pressure level
PNdB	perceived noise decibel
PNL	perceived noise level
P <sub>g</sub> /P <sub>o</sub>	nozzle pressure ratio
V <sub>R</sub>	relative jet velocity
$\theta$	acoustic angle
w <sub>v</sub> /τ	secondary-to-primary corrected weight flow ratio

### References

1. Darchuk, G. V. and Balombin, J. R., "Noise Evaluation of Four Exhaust Nozzles for Afterburning Turbojet Engine," TM X-2014, 1970, NASA, Cleveland, Ohio.
2. Brausch, J. F., "Flight Velocity Influence on Jet Noise of Conical Ejector, Annular Plug and Segmented Suppressor Nozzles," NASA CR-120961, Aug. 1972, General Electric Co., Evendale, Ohio.
3. Groth, H. W., Samanich, N. E., and Blumenthal, P. Z., "Inflight Thrust Measuring System for Underwing Nacelles Installed on a Modified F-106 Aircraft," TM X-2356, 1971, NASA, Cleveland, Ohio.
4. Antl, R. J. and Burley, R. R., "Steady-State Airflow and Afterburning Performance Characteristics of Four J85-GE-13 Turbojet Engines," TM X-1742, 1969, NASA, Cleveland, Ohio.
5. Burley, R. R., "Flight Investigation of Airframe Installation Effects on an Auxiliary Inlet Ejector Nozzle on an Underwing Engine Nacelle," TM X-2396, 1971, NASA, Cleveland, Ohio.
6. Samanich, N. E. and Chamberlin, R., "Flight Investigation of Installation Effects on a Plug Nozzle Installed on an Underwing Nacelle," TM X-2295, 1971, NASA, Cleveland, Ohio.
7. Bresnahan, D. L., "Internal Performance of a 10° Conical Plug Nozzle with a Multispoke Primary and Translating External Shroud," TM X-2573, 1972, NASA, Cleveland, Ohio.
8. Federal Aviation Regulations, Vol. III, Pt. 36, Noise Standards: Aircraft Type Certification, Dept. of Transportation, Federal Aviation Administration, Washington, D.C.
9. Howes, W. L., "Ground Reflections of Jet Noise," TR R-35, 1959, NASA, Cleveland, Ohio.
10. Mangiarotti, R. A.: Doppler Effect Correction for Motions of Source, Observer, and Fluid. D6-17095-TN, AD-669222, Nov. 1966, Renton, Wash.
11. Little, J. W., Miller, R. L., Oncley, P. B., and Pauko, R. E., "Studies of Atmospheric Attenuation of Noise," NASA Acoustically Treated Nacelle Program, SP-220, 1969, NASA Washington, D.C., pp. 125-135.
12. Bishop, D. E. and Franken, P. A., "Propagation of Sound from Aircraft Ground Operations," Progress of NASA Research Relating to Noise Alleviation of Large Subsonic Jet Aircraft, SP-189, 1968, NASA, Washington, D.C., pp. 435-451.

E-7220



Figure 3. - Microphone position and orientation for flyover tests.

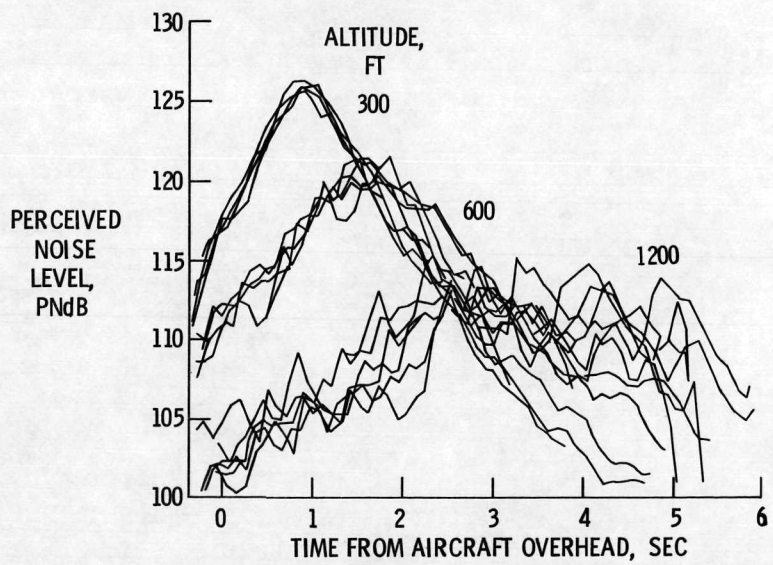
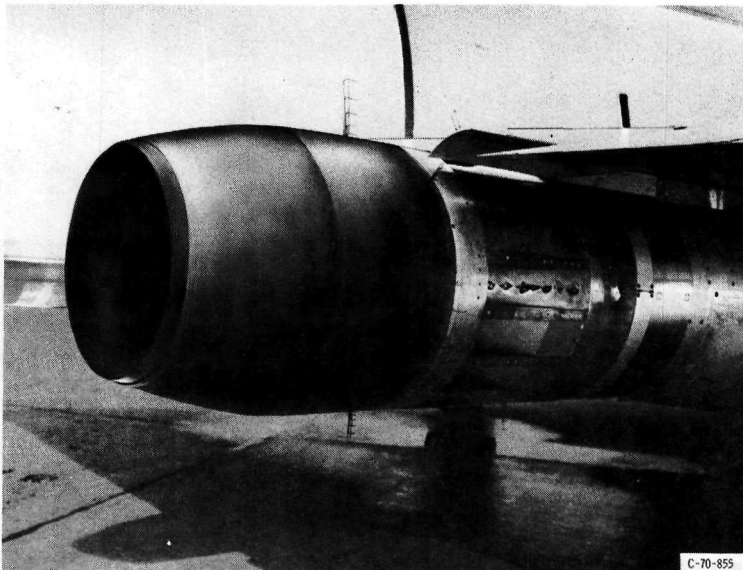


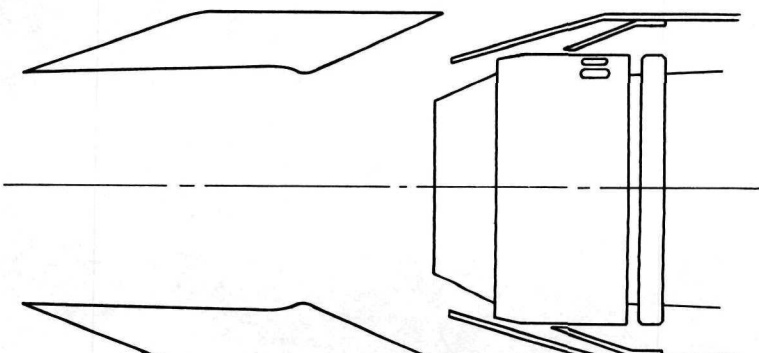
Figure 4. - Repeatability of sound data obtained at various flyover altitudes.



Figure 5. - Microphone position and orientation for static tests.

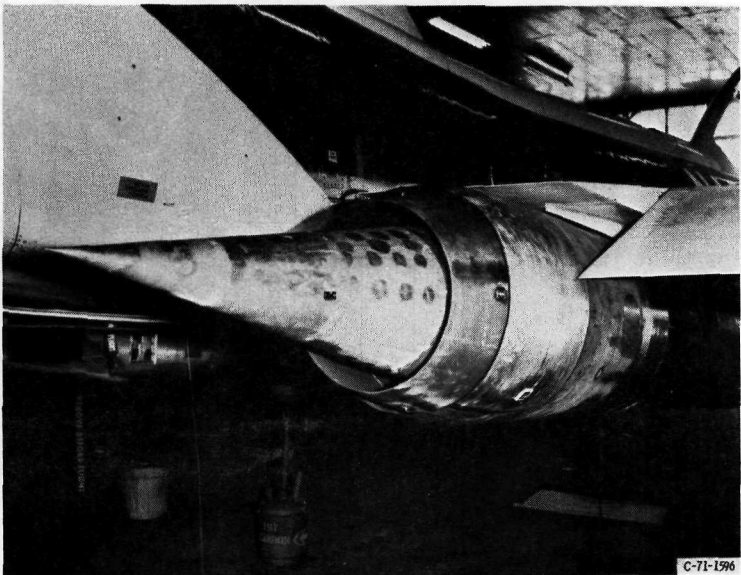


(a) INSTALLED.

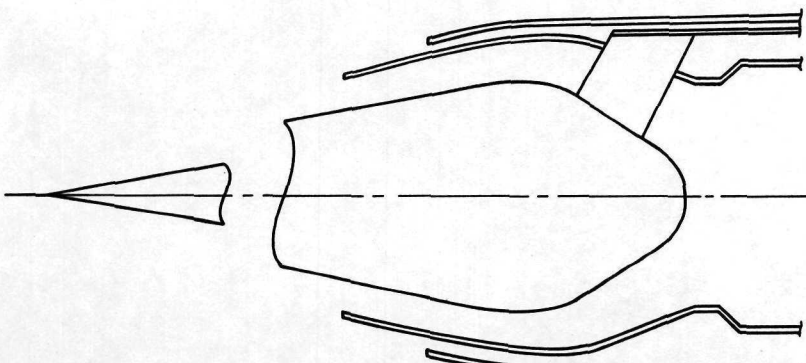


(b) SCHEMATIC.

Figure 6. - Auxiliary inlet ejector nozzle.

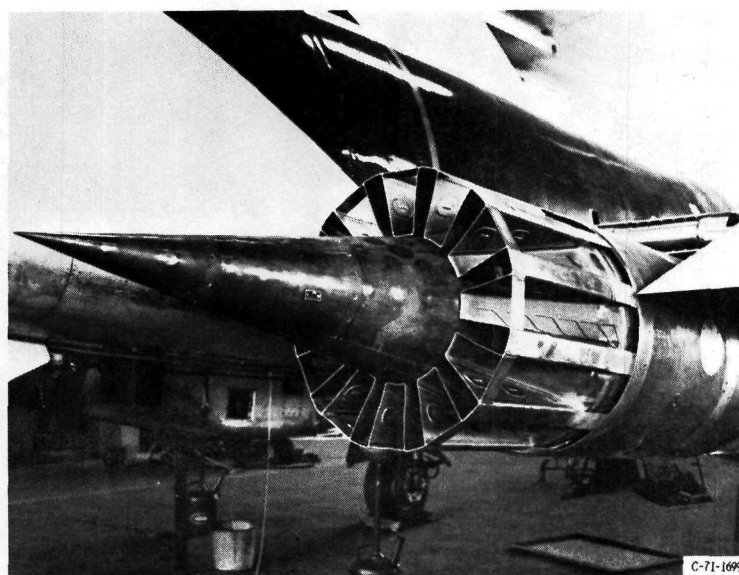


(a) INSTALLED.

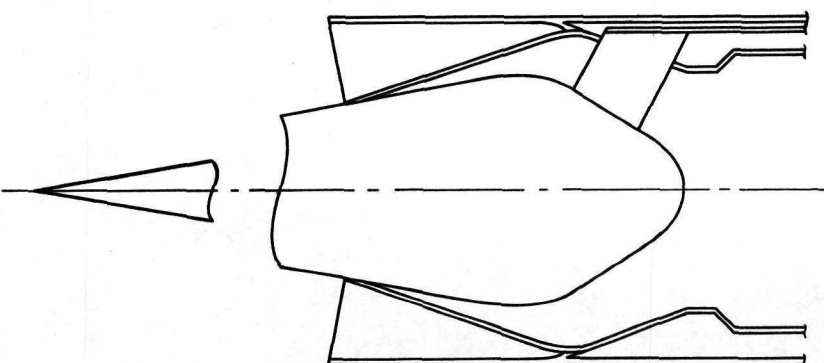


(b) SCHEMATIC.

Figure 7. - Conical plug nozzle.



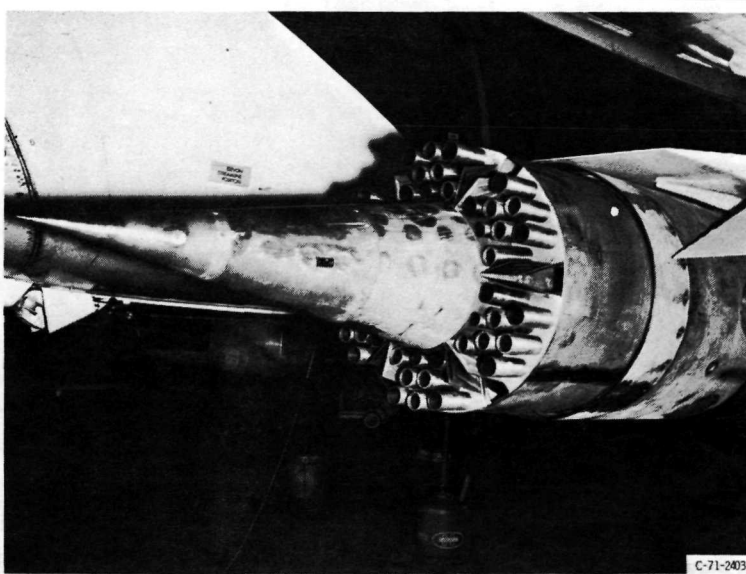
(a) INSTALLED.



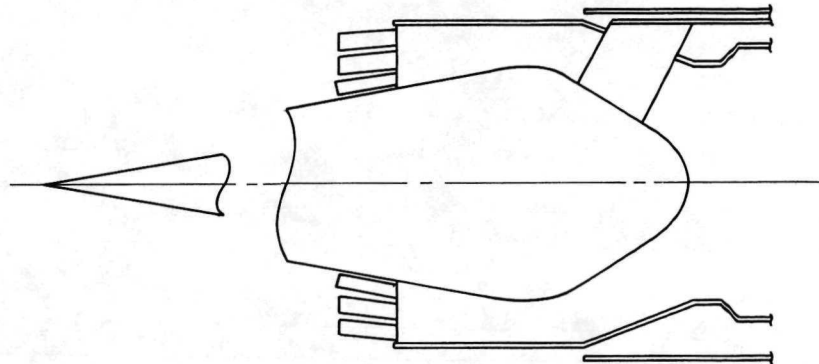
(b) SCHEMATIC.

Figure 8. - 12 chute suppressor nozzle.

E-7220

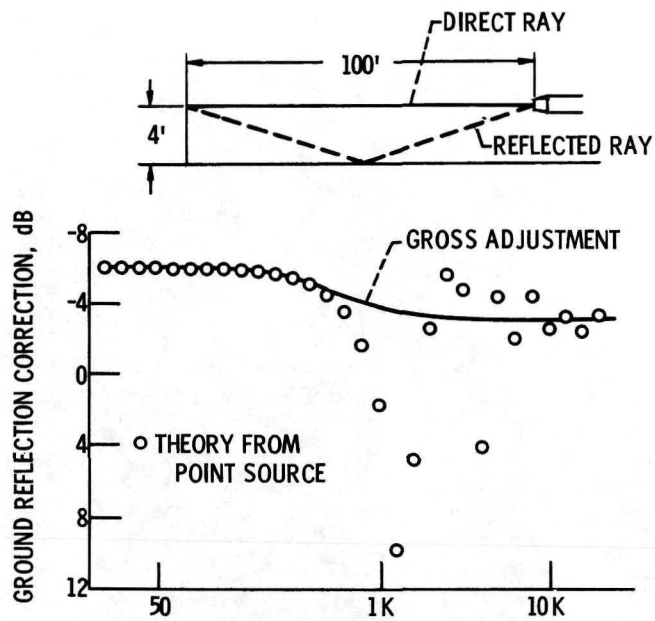


(a) INSTALLED.

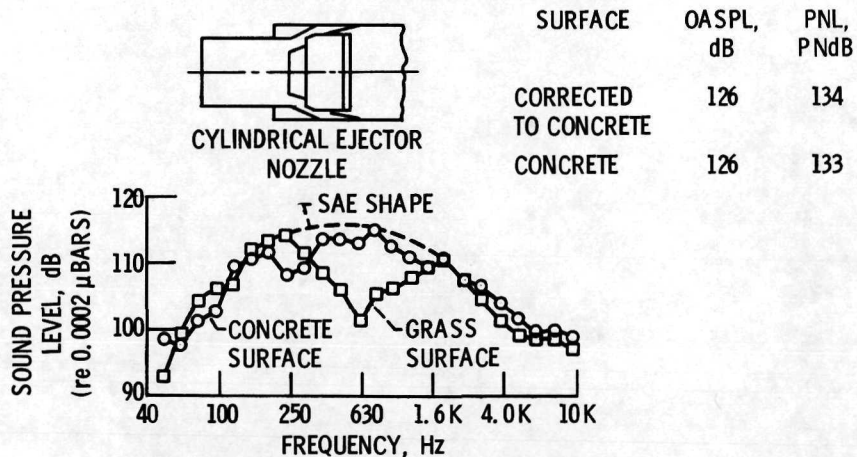


(b) SCHEMATIC.

Figure 9. - 48 tube suppressor nozzle.

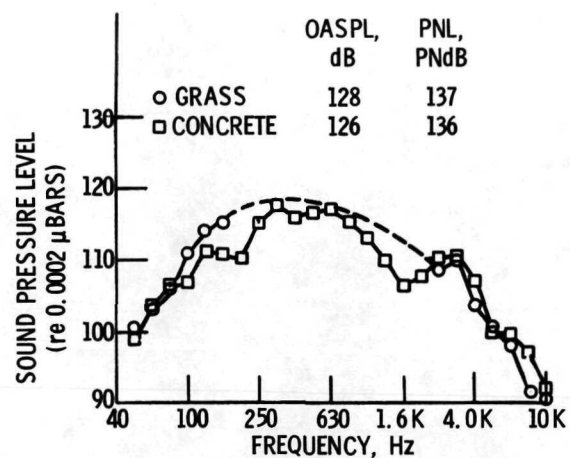


(a) ADJUSTMENT FROM CONCRETE TO FREE-FIELD



(b) ADJUSTMENT FROM GRASS TO CONCRETE SURFACE; CYLINDRICAL EJECTOR NOZZLE.

Figure 10. - Adjustments to measured static spectra; 1/3-octave bands.



(c) COMPARISON OF ADJUSTED STATIC  
SPECTRA TAKEN OVER GRASS AND  
CONCRETE; PLUG NOZZLE;  $\theta = 30^\circ$ .

Figure 10. - Concluded.

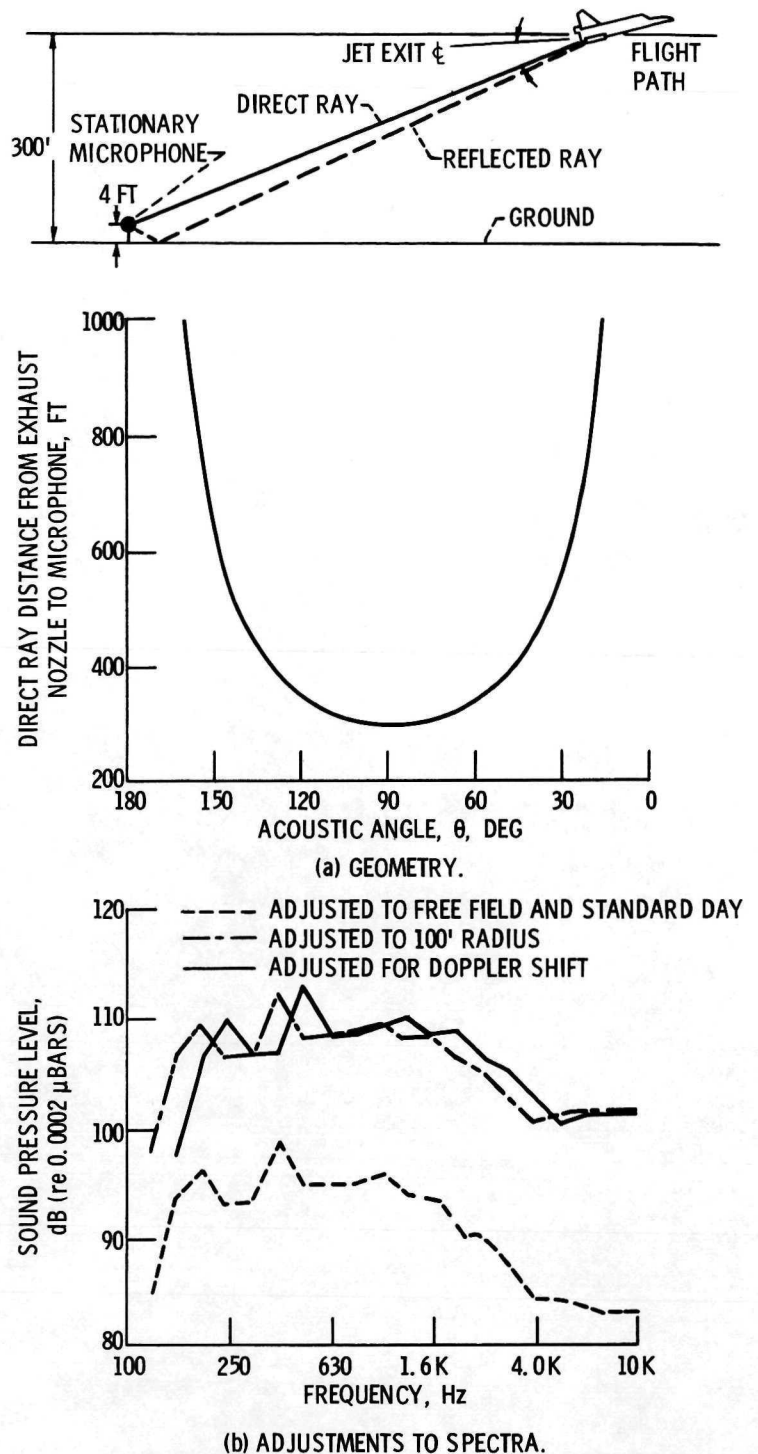


Figure 11. - Flyover geometry and adjustments to spectra; 1/3-octave bands.

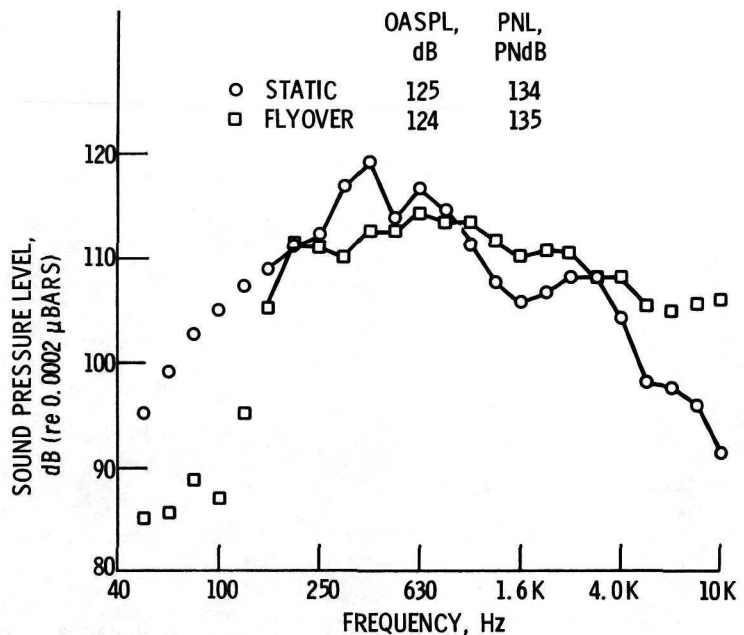


Figure 12. - Comparison of flyover and static spectra for plug nozzle at 100-ft from nozzle.  $V_R = 1970$  FPS;  $\theta = 40^\circ$  (angle of peak noise for flyover). 1/3-octave bands.

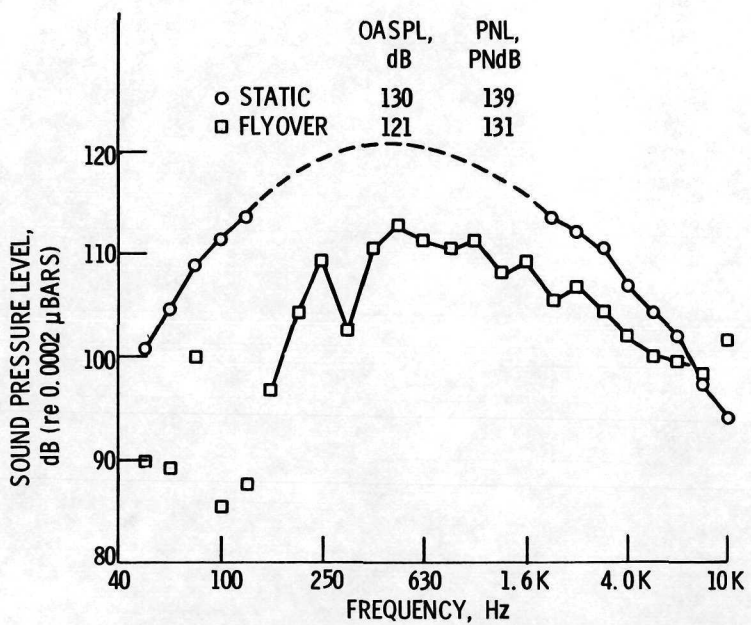


Figure 13. - Comparison of flyover and static spectra for auxiliary inlet ejector nozzle at 100-ft from nozzle.  $V_R = 1970$  FPS;  $\theta = 40^\circ$  (angle of peak noise for flyover). 1/3-octave bands.

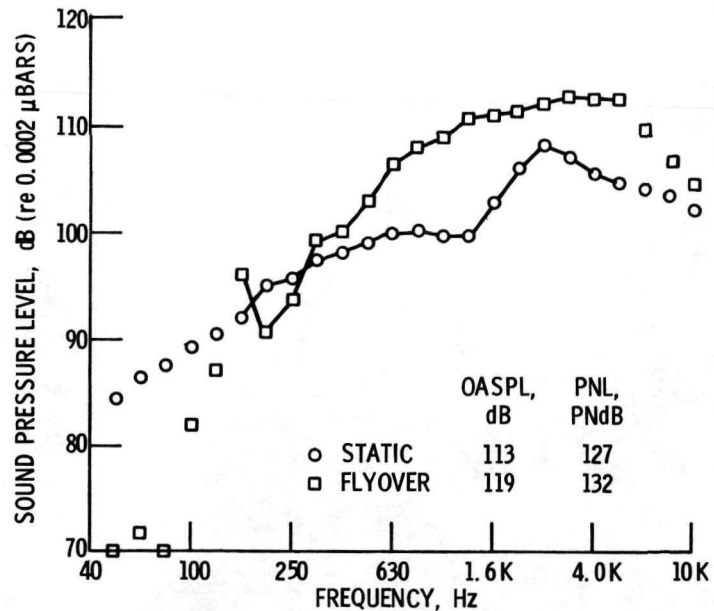


Figure 14. - Comparison of flyover and static spectra for 12-chute suppressor nozzle at 100-ft from nozzle.  
 $V_R = 1970$  FPS;  $\theta = 50^\circ$  (angle of peak noise for flyover).  
 1/3-octave bands.

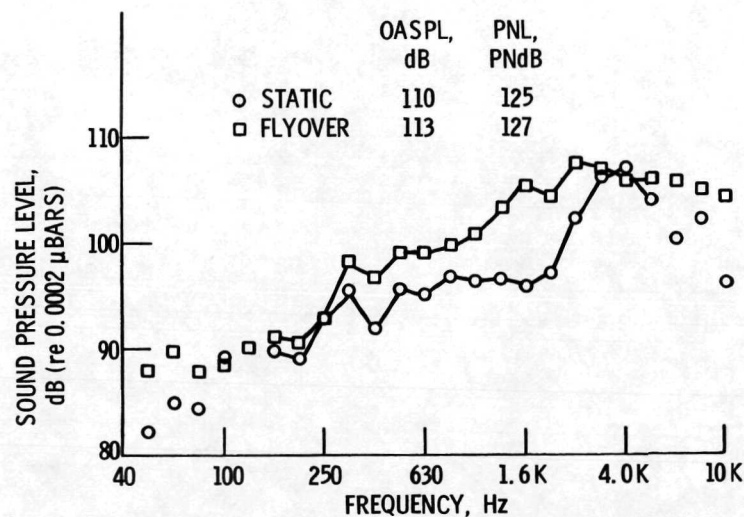


Figure 15. - Comparison of flyover and static spectra for 48-tube suppressor nozzle at 100-ft from nozzle.  $V_R = 1970$  FPS;  $\theta = 70^\circ$  (angle of peak noise for flyover).  
 1/3-octave bands.

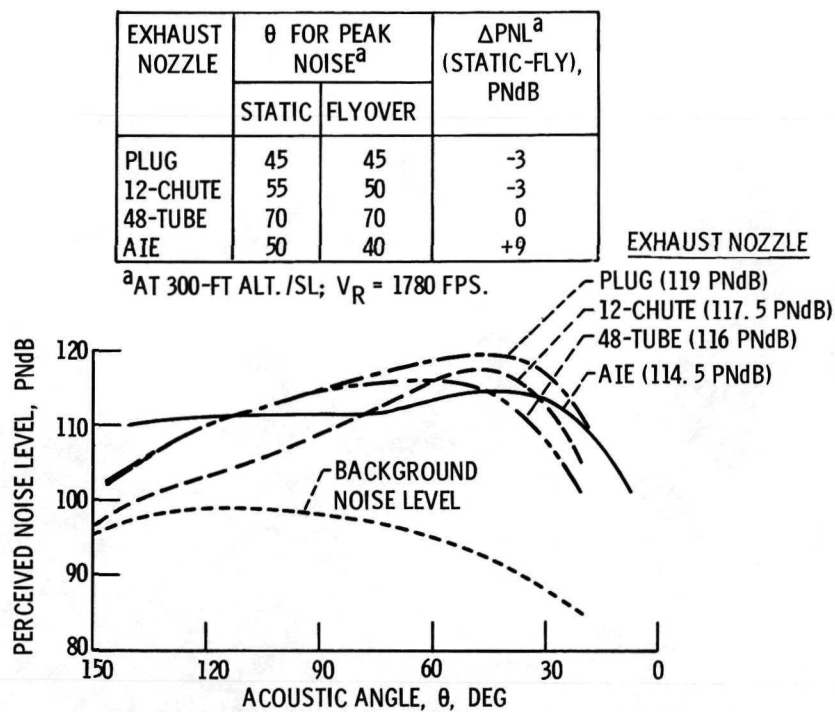


Figure 16. - Flyover noise levels directly beneath flight path. Adjusted to free-field, standard day, and  $V_R = 1780$  FPS.

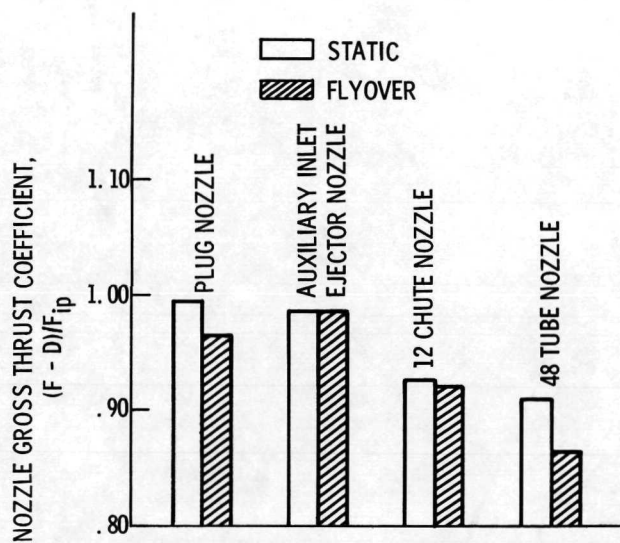


Figure 17. - Thrust performance comparison of the exhaust nozzles.  $(P_g/P_0)_{ST} = 2.0$ ;  $(P_g/P_0)_{FLY} = 2.4$ ,  $\omega\sqrt{\tau} = 0.05$ .